(2)

SECURITY CLASSI

AD-A242 444

JMENTATION PAGE

1a. REPORT SEC: Unclassifi	1b. RESTRICTIVE MARKINGS
2a. SECURITY CLA	3. DISTRIBUTION/AVAILABILITY OF REPORT: Unclassified/Unlimited
2b. DECLASSIFICATION/DOWNGRADING SCHEDU	
4. PERFORMING ORGANIZATION REPORT NUMBER(S): ONR Technical Report 3	5. MONITORING ORGANIZATION REPORT NUMBER(S)
6a. NAME OF PERFORMING ORGANIZATION: Dept of Chemical Engineering and Materials Science; 6b. OFFICE SYMBOL (If applicable): Code 1113	7a. NAME OF MONITORING ORGANIZATION: Office of Naval Research
6c. ADDRESS (City, State, and ZIP Code): University of Minnesota Minneapolis, MN 55455	7b. ADDRESS (City, State, and ZIP Code): 800 North Quincy Street Arlington, VA 22217
8a. NAME OF FUNDING/SPONSORING ORGANIZATION: Office of Naval Research; 8b. OFFICE SYMBOL (If applicable)	9. PROCUREMENT INSTRUMENT IDENTIFICATION NUMBER: Contract No. N00014 91-J-1927
8c. ADDRESS (City, State, and ZIP Code): 800 North Quincy Street Arlington, VA 22217-5000	10. SOURCE OF FUNDING NUMBERS: PROGRAM ELEMENT NO. / PROJECT NO. / TASK NO. / WORK UNIT ACCESSION NO

11. TITLE (Include Security Classification)
Effect of Comproportionation on the Voltammetric Reduction of Methyl Viologen in Low Ionic Strength Solutions

12. PERSONAL AUTHOR(S)
John D. Norton and Henry S. White

13a. TYPE OF REPORT	13b. TIME COVERED	14. DATE OF REPORT (Year, Month, Day)	15. PAGE COUNT
Technical	FROM 1/1/91 TO 10/31/93	November 10, 1991	17 pages

16. SUPPLEMENTARY NOTATION
submitted for publication in the Journal of Electroanalytical Chemistry

17. COSATI CODES			18. SUBJECT TERMS (Continue on reverse if necessary and identify by block number)
FIELD	GROUP	SUB-GROUP	methylviologen, migration, homogeneous comproportionation

19. ABSTRACT (Continue on reverse if necessary and identify by block number)

Voltammetric studies of the sequential reduction of methyl viologen (MV^{+2}) in acetonitrile solutions are reported.

$$MV^{+2} + e^- \longrightarrow MV^+ \qquad MV^+ + e^- \longrightarrow MV$$

The rate at which MV^{+2} is electrochemically reduced is governed by diffusion and migration. We demonstrate, using numerical simulations, that the homogeneous conproportionation,

$MV^{+2} + MV \xrightarrow{k_b} 2MV^+$ which is coupled to the electrochemical generation of MV, reduces the electric field within the depletion layer in low ionic strength solutions, thereby decreasing the migrational flux of MV^{+2}. We show that the local electric field within the depletion layer is a function of the homogeneous electron-transfer rate constant, k_b. Analysis of experimental limiting currents as a function of the supporting electrolyte concentration yields a lower limit of $k_b \geq 3 \times 10^7\ M^{-1}s^{-1}$.

20. DISTRIBUTION/AVAILABILITY OF ABSTRACT	21. ABSTRACT SECURITY CLASSIFICATION
☒ UNCLASSIFIED/UNLIMITED ☐ SAME AS RPT ☐ DTIC USERS	Unclassified
22a. NAME OF RESPONSIBLE INDIVIDUAL: Henry S. White	22b. TELEPHONE (Include Area Code): (612) 625-6345; 22c. OFFICE SYMBOL

DD FORM 1473, 84 MAR — 83 APR edition may be used until exhausted. All other editions are obsolete. SECURITY CLASSIFICATION OF THIS PAGE

OFFICE OF NAVAL RESEARCH

Contract N00014-91-J-1927

R&T Code 413v001

Technical Report No. 3

EFFECT OF COMPROPORTIONATION ON THE VOLTAMMETRIC REDUCTION OF METHYL VIOLOGEN IN LOW IONIC STRENGTH SOLUTIONS

by

JOHN D. NORTON AND HENRY S. WHITE

Prepared for Publication in the

JOURNAL OF ELECTROANALYTICAL CHEMISTRY

University of Minnesota
Department of Chemical Engineering and Materials Science
Minneapolis, MN 55455

November 10, 1991

Submitted to *J. Electroanalytical Chem.*, May, 1991
Revised September, 1991

Effect of Comproportionation on the Voltammetric Reduction of Methyl Viologen in Low Ionic Strength Solutions

John D. Norton and Henry S. White
Department of Chemical Engineering and Materials Science
University of Minnesota
Minneapolis, MN 55455

INTRODUCTION.

A variety of electrochemical methods are available for investigating homogeneous chemical reactions coupled to an initial electron-transfer step (1-4). Frequently, these methods are based on varying the mass-transfer rate(s) of reactant or intermediate(s) relative to the rate of chemical reaction. In a recent report (5), we proposed a new general method using microelectrodes (6-11), in low ionic strength solutions (11-21), that allows controlled variation of the mass-transfer coefficients of *charged* reactants and intermediates through the influence of electric fields. This strategy was employed in a preliminary investigation of electron transfer reactions of the general form:

$$A^z + e^- \longrightarrow A^{z-1} \qquad (1)$$

$$A^{z-1} + e^- \longrightarrow A^{z-2} \qquad (2)$$

$$A^{z-2} + A^z \xrightarrow{k_b} 2A^{z-1} \qquad (3)$$

where reactions (1) and (2) represent the sequential 1-e^- reductions of a soluble electroactive species, A^z, at the electrode surface. For redox systems in which the formal potentials of reactions

(1) and (2) are separated by several tenths of a volt, ($E^{o'}(A^{z/z-1}) > E^{o'}(A^{z-1/z-2})$), the thermodynamically-favored comproportionation of A^{z-2} and A^{z} (reaction (3)) generates the singly-reduced intermediate A^{z-1} at potentials corresponding to the overall 2-e$^-$ reduction of A^{z}. If the comproportionation reaction yields an ionic species, $z-1 \neq 0$, mass-transport of A^{z-1} by migration may be strongly influenced by electric fields within the depletion layer that result from the depletion or generation of ionic species in the faradaic processes (reactions (1) and (2)). Thus, the transport of the chemical intermediate A^{z-1} towards (or away from) the electrode can be accelerated or retarded by varying the concentration of supporting electrolyte added to the solution. Conversely, the homogeneous generation of an ionic species may increase or decrease the electric field within the depletion layer, thereby accelerating or retarding the flux of the bulk reactant species (A^{z}) to the electrode. These effects are enhanced in low ionic strength solutions and, with the recent advent of microelectrode techniques, can be quantitatively investigated (22). For example, digital simulations and experimental investigations (5) demonstrate that the magnitude of the limiting current of the second wave observed in the sequential 2-e$^-$ reduction of tetracyanoquinodimethane (TCNQ), $z = 0$, at Pt microdisk electrodes in acetonitrile varies from a purely diffusion controlled value in solutions containing excess supporting electrolyte ($C_{elec}/C_{redox} >> 1$) to 42% of the diffusion-limited value in solutions in which the concentration of TCNQ exceeds that of the supporting electrolyte ($C_{elec}/C_{redox} << 1$). The dependence of the magnitude of the second wave on electrolyte concentration is due to migration of $TCNQ^-$ generated by comproportionation of the parent compound (TCNQ) and the 2-e$^-$ reduction product ($TCNQ^{-2}$), reaction (3). The comproportionation rate constant, k_b, can be determined from measurement of the steady-state limiting current as a function of electrolyte concentration. A similar behavior was observed in the voltammetric oxidation of tetrathiafulvalene, TTF.

In this report we describe the 1- and 2-e$^-$ reductions of methyl viologen (MV^{+2}) in acetonitrile as a function of electrolyte concentration. We show that the limiting current for the 2-e$^-$ reduction of MV^{+2} in low ionic strength *increases* with decreasing electrolyte concentrations, but at a smaller rate than predicted based solely on mass-transport considerations. Experimentation and analyses of the coupling of diffusional-migrational transport and chemical reaction of an ionic

reactant, e.g., MV^{+2}, is significantly more complex than previously encountered in similar investigations of neutral parent species (TTF or TCNQ) due to (i) the increased role of migration in determining the overall flux of an ionic reactant, and (ii) the smaller working range of total solution ionic strength that can be explored for investigating migrational currents. In spite of these difficulties, our findings are in accord with the general mechanism proposed above and provide a lower limit of the bimolecular electron-transfer rate constant, k_b, for the comproportionation of MV^{+2} and electrogenerated MV, eq. (3).

EXPERIMENTAL.

N,N'-dimethyl-4,4'-bipyridinium hexafluorophosphate, $MV(PF_6)_2$, was prepared by metathesis of the corresponding chloride salt (K & K Laboratories) with ammonium hexafluorophosphate (Sigma). The resulting precipitate was washed with H_2O and dried. Acetonitrile (Fisher) was dried over activated 4 Å molecular sieves. Tetra-n-butylammonium perchlorate (TBAP, Southwestern Analytical) was recrystallized 3 times from ethyl acetate and dried under vacuum.

Pt microdisk electrodes were prepared as previously described (23). A 2 cm length of a nominally 12.5 μm radius Pt wire (Goodfellow, 99.99%) was attached to the end of a copper wire with Ag paint (Acme) and subsequently encased in the tip of a glass pipet with epoxy ("white epoxi-patch", Dexter Corp., Olean, NY). The tip of the electrode was ground flat with 600 grit emery paper to expose the cross-section of the Pt wire.

Electrochemical measurements were made using a conventional three-electrode cell. A sodium saturated calomel electrode (SSCE) was used as the reference electrode. Voltammetric curves were obtained using a Princeton Applied Research Corp. Model 173 potentiostat and Model 175 Universal Programmer. Solutions were purged with N_2 prior to each experiment.

Computer simulations utilized a finite-difference method with an exponentially expanding space grid (24,25) to simulate the time dependent flux and spatial distribution of electrolyte and redox species at a hemispherical electrode of radius, r_o. A large, concentric, hemispherical counter electrode was assumed, which maintained a radial flux of ions to the microelectrode at all times.

Initially, the reactant (MV^{+2}), its counter ion (PF_6^-) and the supporting electrolyte (TBAP), if present, were assumed to exist at their respective uniform bulk concentrations. Numerical calculation of the limiting current for the 1-e^- reduction of MV^{+2} (rxn. (1)) was performed by setting the surface concentration of MV^{+2} to zero at t = 0, and calculating the time-dependent, diffusion-migration flux of MV^{+2} to the electrode. Transport of all species was assumed to be described by the Nernst-Planck equation. For the overall 2-e^- reduction of MV^{+2} (rxn. (2)), the surface concentrations of both reactant (MV^{+2}) and intermediate species (MV^+) were set equal to zero and the diffusion-migration current calculated as describe above. The homogeneous bimolecular reaction between MV^{+2} and MV (rxn. (3)) was incorporated in the simulation using previously described methods (4,5). The simulation yielded the limiting current for the 1- and 2-e^- processes normalized to that of a purely diffusion-limited 1-e^- reaction, $i_{1(diff.)}$. The time-dependent electric field was calculated from the local ion concentration after each time increment using the expression previously reported (26). Simulations were allowed to run until the normalized limiting current changed by less than 0.01 % per unit of dimensionless time, $\tau = Dt/r_o^2$. This was accomplished in all cases for $\tau < 10$. Simulations were performed using an HP 375CH computer.

RESULTS.

For reaction at a microdisk electrode involving the transfer of n electrons, the diffusion limited current is

$$i_{n(diff.)} = 4nFDC^*r_o \qquad (4)$$

where F is Faraday's constant, D and C^* are the bulk diffusivity and concentration, respectively, of the reactant, and r_o is the electrode radius. Figure 1 shows representative voltammograms obtained for the two sequential 1-e^- reductions of 0.5 mM MV^{+2} in acetonitrile at a 12.5 μm radius Pt microdisk electrode. Figures 1A - 1C correspond to supporting electrolyte (TBAP) concentrations of 10 mM, 0.5 mM and 0 mM, respectively. In the presence of excess supporting

electrolyte, $C_{elec}/C_{redox} >> 1$ (10 mM TBAP, Fig. 1A), the transport-limited current for the 2-e$^-$ reduction of MV^{+2} is twice that for the 1-e$^-$ reduction, as expected for a diffusion controlled reaction, eq. (4) (i.e., $i_{2(diff.)} = 2i_{1(diff.)}$). Analysis of the limiting currents for the 1- and overall 2-e$^-$ reductions in the presence of 10 mM TBAP yields a MV^{+2} diffusivity of $D = (2.0 \pm 0.1) \times 10^{-5}$ cm^2/s.

As the concentration of TBAP is decreased (Fig. B and C), the limiting currents for both the 1- and 2-e$^-$ reductions increase due to migration of MV^{+2} to the electrode surface. Migration of MV^{+2} towards the electrode surface results from the steady-state electric field that is generated within the depletion layer by reduction of the dication (MV^{+2}) to either the monocation (MV^+) or the neutral species (MV) (22). For a TBAP concentration of 0.5 mM, C_{elec}/C_{redox}, the limiting current of the 1-e$^-$ reduction increases to 1.2 times its diffusion limited value, $i_{1(diff.)}$, and the limiting current for the 2-e$^-$ reduction increases to $2.8i_{1(diff.)}$. When no supporting electrolyte is intentionally added to the solution, C_{elec}/C_{redox}, the corresponding values are $1.3i_{1(diff.)}$ and $4.0i_{1(diff.)}$. The transport limited currents for the 1- and 2-e$^-$ reductions of MV^{+2}, normalized to $i_{1(diff.)}$, are shown in Figure 2 as a function of the ratio of the supporting electrolyte concentration to the redox concentration (C_{elec}/C_{redox}) for a range of supporting electrolyte concentrations of over 10^3, not including measurements made in the absence of intentionally added supporting electrolyte.

DISCUSSION.

In the absence of coupled homogeneous reactions, the steady-state limiting currents obtained in voltammetric experiments for the two sequential 1-e$^-$ reductions of MV^{+2} at a microdisk electrode are anticipated to be determined by diffusion and migration of MV^{+2} to the electrode surface. In the presence of excess supporting electrolyte ($C_{elec}/C_{redox} >> 1$), the electric fields in solution are negligible and the steady-state currents will be limited by diffusion of MV^{+2} to the electrode surface. As such, the steady-state current of the overall 2-e$^-$ reduction of MV^{+2} is expected to be twice that for the 1-e$^-$ reduction, as experimentally observed (Figure 1A). In solutions in which the concentration of supporting electrolyte is less than that of the redox species ($C_{elec}/C_{redox} << 1$), significant electric fields exist within the depletion layer and transport of MV^{+2}

to the electrode surface is controlled by both diffusion and migration (15, 20, 22). For a spherical electrode, Amatore et al. (16) have shown that in such situations the limiting current corrected for effects of migration is:

$$\frac{i_n}{i_{n(diff.)}} = 1 \pm z\{1 + (1 + |z|)(1 - z/n)\ln(1 - 1/[(1 + |z|)(1 - z/n)])\} \qquad (5)$$

for $n \neq z$ and

$$\frac{i_n}{i_{n(diff.)}} = 1 + |n| \qquad (6)$$

for $n = z$. (The sign used in eq. (5) is negative for $n > z$ and positive for $n < z$.)

Noting that the mass-transport limited current at a microdisk can be approximated to that at a hemisphere of equal area (6,20), it is interesting to apply eqs. (5) and (6) to the sequential 1-e^- voltammetric reductions of MV^{+2}, a case where $z = +2$ and $n = 1$ and 2. For Fig. 1C, eq. (5) predicts the limiting current for the 1-e^- reduction will be $1.27i_{l(diff.)}$, in excellent agreement with our results ($1.3i_{l(diff.)}$). However, for the 2-e^- reduction in Fig. 1C, eq. (6) predicts a limiting current of $6.0i_{l(diff.)}$, which is 50% larger than the experimentally obtained value of $4.0i_{l(diff.)}$. Thus, migration alone can not account for the dependence of the limiting current of the second wave on TBAP concentration.

To explain the effect of electrolyte concentration on the transport-limited current of the 2-e^- reduction of MV^{+2}, we consider the effects of the coupled comproportionation of MV^{+2} and MV in solution to form MV^+. The equilibrium constant of comproportionation, $K_{eq} = \exp\{(F/RT)(\Delta E^{o'})\} = 8.5 \times 10^6$, can be obtained from the difference, $\Delta E^{o'}$, between the formal potentials of the first ($E^{o'} = 0.4$ V vs SSCE) and second ($E^{o'} = 0.81$ V vs SSCE) electron-transfer reactions as measured from the voltammetric waves in the presence of excess supporting electrolyte (Figure 1A). The comproportionation of MV and MV^{+2} is a simple 1-e^-, homogeneous electron-transfer reaction and is reported to be essentially diffusion controlled ($\sim 3 \times 10^9$ $M^{-1}s^{-1}$)(27,28).

Simulated values of the steady-state limiting currents for the 1-e⁻ reduction (i_1) and the 2-e⁻ reduction (i_2), normalized to the diffusion-limited current of the 1-e⁻ reduction in the presence of excess supporting electrolyte ($i_{1(diff.)}$), are shown in Figure 2 for several values of the dimensionless rate constant k^*, and compared to the voltammetric data over a wide range of C_{elec}/C_{redox}. The dimensionless rate constant k^* ($= k_b r_o^2 C_{redox}/D$) represents the rate of bimolecular comproportionation within the depletion layer ($k_b r_o C_{redox}$) relative to the rate of mass-transport (D/r_o) (5).

For very small values of k^* ($\leq 10^{-3}$), the rate of comproportionation of MV and MV^{+2} is negligible relative to the rate of mass-transport, and the simulation predicts a behavior identical to the purely transport controlled behavior described by Amatore and coworkers (16), i.e., $i_1 = i_{1(diff.)}$ and $i_2 = 2i_{1(diff.)}$ in the presence of excess supporting electrolyte, and $i_1 = 1.27i_{1(diff.)}$ and $i_2 = 6.0i_{1(diff.)}$ in the absence of excess supporting electrolyte. Simulated concentration profiles of MV and MV^{+2} at an electrode potential corresponding to the limiting current plateau of the second reduction wave are shown in Figure 3 for solutions containing excess (Fig. 3A) and no added supporting electrolyte (Fig. 3B). The increased electric field in the absence of supporting electrolyte is clearly reflected in Fig. 3B by the marked increase in the concentration of MV within the depletion layer relative to that shown in Fig. 3A. For increasing values of k^*, a substantial amount of MV^+ is produced by homogeneous reaction within the depletion layer, as shown in Figures 3C and 3D. When excess supporting electrolyte is present there is no significant electric field in the solution and diffusion governs the transport of all species (Fig. 3C). In this case, the reaction has no effect on the observed current as diffusion controls the transport of the MV^+ generated in solution. A simple mass balance of eqs. (1) - (3) demonstrates that, in this limit, one-half of chemically generated MV^+ is transported to the electrode surface and one-half transported to the bulk solution. However, when little or no supporting electrolyte is present in solution, a significant electric field exists in solution, and the flux of chemically generated MV^+ and bulk MV^{+2} to the electrode surface is enhanced by migration (Fig. 3D). The chemical generation of positively charged MV^+ in solution results in a smaller field than would be expected in the absence of reaction (3) thereby reducing the migrational flux of MV^{+2}, Fig. 4. The magnitude of the 2-e⁻

reduction wave is correspondingly smaller than would be observed in the absence of reaction. Very good agreement is found between the experimental and simulated currents (Fig. 2) for $k^* \geq 10^3$, corresponding to a comproportionation rate constant $k_b \geq 3 \times 10^7\ M^{-1}s^{-1}$ (using r_o = 12.5 μm, C_{redox} = 0.5 mM, and $D = 2.0 \times 10^{-5}\ cm^2/s$). Similarly, the experimental values of the magnitude of first reduction wave of MV^{+2} (reaction (1)), which is not influenced by coupled chemical reactions are in excellent agreement with numerical simulations over a 3 order-of-magnitude range in C_{elec}/C_{redox}.

An interesting but separate conclusion of this work concerns the question of whether the overall 2-e^- reduction of a MV^{+2} species occurs as a single 2-e^- transfer process or as two sequential 1-e^- transfers. Fig. 3 clearly shows that at a hemi-spherical microelectrode the concentration of MV^{+2} falls to negligible values at a distance of ~1 - $2r_o$ from the electrode surface for $k^* \geq 10^3$, regardless of the supporting electrolyte concentration. In the present experiments, this distance corresponds to 12 -25 μm, assuming the approximation of a microdisk by a hemi-spherical geometry. Thus, for moderate to diffusion-controlled comproportionation rates (i.e., $k^* \geq 10^3$), the only heterogeneous reactions involved in the *steady-state* reduction of MV^{+2} is the 1-e^- reduction of the monocation MV^+ (rxn. 2). This finding completely circumvents the issue of a 2-e^- vs. a 2 sequential 1-e^- transfer mechanism.

CONCLUSION.

In our previous work, it was noted that control of electric fields within the depletion layer by variation of the supporting electrolyte concentration could be applied to analyze many different coupled homogeneous reactions. The observed dependence of limiting currents on supporting electrolyte concentration is strongly affected by the specific charges of the chemical species involved in the electrochemical reaction. For the reduction or oxidation of a neutral species (e.g., TCNQ or TTF, z = 0), a decrease in the supporting electrolyte concentration leads to a decrease in the magnitude of the second reduction wave with respect to the first. In the present analysis of the reduction of MV^{+2}, the magnitude of the second reduction wave *increases* with respect to the first with decreasing supporting electrolyte concentration, but at a slower rate than predicted by

consideration of migration alone. This highly specific dependence of voltammetric currents on the electrolyte concentration, on the rates of coupled chemical reactions, and on the charge(s) of the species involved in coupled chemical reactions, may provide a general means for the elucidation of the mechanisms involved in homogeneous reactions coupled to an electron-transfer reaction.

As a final note, it should be emphasized that the above analyses apply only to steady-state voltammetric currents. The transient current at a microelectrode in a fast-sweep voltammetric experiment or in a potential step chronoamperometric measurement will also be affected by generation and migration of ionic intermediates produced via homogeneous chemical reactions. However, the electric fields within the depletion layer will develop and approach steady-state at the same rate as both the concentration profiles and the measured current. Thus, the migrational component of the overall molecular flux will be time-dependent. Consequently, the ratio of the transient currents in the presence and absence of supporting electrolyte will be time-dependent, yielding the limiting steady-state values reported in this article at long times.

REFERENCES.

1. J. Koutecky and V. G. Levich *Zh. Fiz. Khim.* 32 (1958) 1565.
2. S. Bruckenstein and B. Miller *Accts. Chem. Res.* 10 (1977) 54.
3. R. S. Nicholson and I. Shein *Anal. Chem.* 36 (1964) 706.
4. A. J. Bard and L. R. Faulkner *Electrochemical Methods*, Wiley, New York, 1980 and references within.
5. J. D. Norton, W. E. Benson, H. S. White, B. D. Pendley and H. D. Abruña submitted to *Anal. Chem.* November, 1990.
6. M. Fleischmann, F. Lasserre, J. Robinson and D. Swan *J. Electroanal. Chem.* 177 (1984) 97.
7. M. Fleischmann, F. Lasserre and J. Robinson *J. Electroanal. Chem.* 177 (1984) 115.
8. G. Denault, M. Fleischmann, D. Pletcher and O. R. Turry *J. Electroanal. Chem.* 280 (1990) 243.
9. L. Geng and R. W. Murray *Inorg. Chem.* 25 (1986) 3115.
10. C. L. Miaw, J. F. Rusling and A. Owlia *Anal. Chem.* 62 (1990) 268.
11. J. O. Howell and R. M. Wightman *J. Phys. Chem.* 88 (1984) 3915.
12. J. Cassidy, S. B. Khoo, S. Pons and M. Fleischmann *J. Phys. Chem.* 89 (1985) 3933.
13. T. Dibble, S. Bandyopadhyay, J. Ghoroghchian, J. J. Smith, F. Sarfarazi, M. Fleischmann and S. Pons *J. Phys. Chem.* 90 (1986) 5275.
14. M. Ciszkowska, Z. Stojek and J. Osteryoung *Anal. Chem.* 62 (1990) 349.
15. A. M. Bond, M. Fleischmann and J. Robinson *J. Electroanal. Chem.* 168 (1984) 299.
16. C. Amatore, B. Fosset, J. Bartlet, M. R. Deakin and R. M. Wightman *J. Electroanal. Chem.* 256 (1988) 255.
17. A. M. Bond and P. A. Lay *J. Electroanal. Chem.* 199 (1986) 285.
18. M. J. Peña, M. Fleischmann and N. Garrard *J. Electroanal. Chem.* 220 (1987) 31.
19. C. Amatore, M. R. Deakin and R. M. Wightman *J. Electroanal. Chem.* 220 (1987) 49.
20. A. M. Bond, M. Fleischmann and J. Robinson *J. Electroanal. Chem.* 172 (1984) 11.
21. K. B. Oldham *J. Electroanal. Chem.* 122 (1981) 1.

22. K. B. Oldham *J. Electroanal. Chem.* 250 (1988) 1.

23. R. A. Malmsten, C. P. Smith and H. S. White *J. Electroanal. Chem.* 215 (1986) 223.

24. S. W. Feldberg *J. Electroanal. Chem.* 127 (1981) 1.

25. T. Joslin and D. Pletcher *J. Electroanal. Chem.* 49 (1974) 171.

26. J. D. Norton, H. S. White and S. W. Feldberg *J. Phys. Chem.* 94 (1990) 6772.

27. D. R. Rosseinsky and P. M. S. Monk, *Chem. Soc. Faraday Trans.* 86 (1990) 3597.

28. N. Winograd and T. Kuwana, J. Am. Chem. Soc. 92 (1970) 224.

FIGURES.

1. Cyclic voltammograms for the reduction of 0.5 m$\underline{M}$ MV^{+2} in acetonitrile at a 12.5 μm radius Pt disk electrode. Concentration of supporting electrolyte (TBAP): (A) 10 m$\underline{M}$; (B) 0.5 m$\underline{M}$; (C) 0 m$\underline{M}$. The solutions were purged with N_2.

2. Limiting currents for the 1-e⁻ and 2-e⁻ reductions of MV^{+2} normalized to the diffusion-limited current of the 1-e⁻ reduction in the presence of excess supporting electrolyte ($i_{1(diff.)}$) as a function of C_{elec}/C_{redox} and k^* ($= k_b r_o^2 C_{redox}/D$). Solid lines correspond to computer-simulated values. Circles correspond to experimental values obtained in 0.5 m$\underline{M}$ MV^{+2} acetonitrile solutions containing TBAP as supporting electrolyte. The data points labeled "no supporting electrolyte" are plotted on the abscissa at an arbitrarily small value of C_{elec}/C_{redox}.

3. Simulated concentrations profiles of MV and MV^+ as a function of C_{elec}/C_{redox} and k^*. (A): $C_{elec}/C_{redox} = 20$, $k^* \leq 10^{-3}$; (B): $C_{elec}/C_{redox} = 0$, $k^* \leq 10^{-3}$; (C): $C_{elec}/C_{redox} = 20$, $k^* \geq 10^3$; (D): $C_{elec}/C_{redox} = 0$, $k^* \geq 10^3$. Profiles correspond to an electrode potential sufficiently negative to cause the overall 2-e⁻ reduction of MV^{+2} at mass-transfer controlled rates. The concentrations of each species are normalized to the bulk solution concentration of MV^{+2}, C_{redox}. The distance from the electrode surface is normalized to the electrode radius, r_o.

4. Dependence of the ratio of electric fields, $E(k^* \geq 10^3)/E(k^* \leq 10^{-3})$ on distance from electrode surface. The insert shows simulated values of E with ($k^* \geq 10^3$) and without ($k^* \leq 10^{-3}$) inclusion of the comproportionation reaction of MV and MV^{+2}. Profiles correspond to an electrode potential sufficiently negative to cause the 2-e⁻ reduction of MV^{+2} at mass-transfer controlled rates. Distance from the electrode surface is normalized to the electrode radius, r_o.

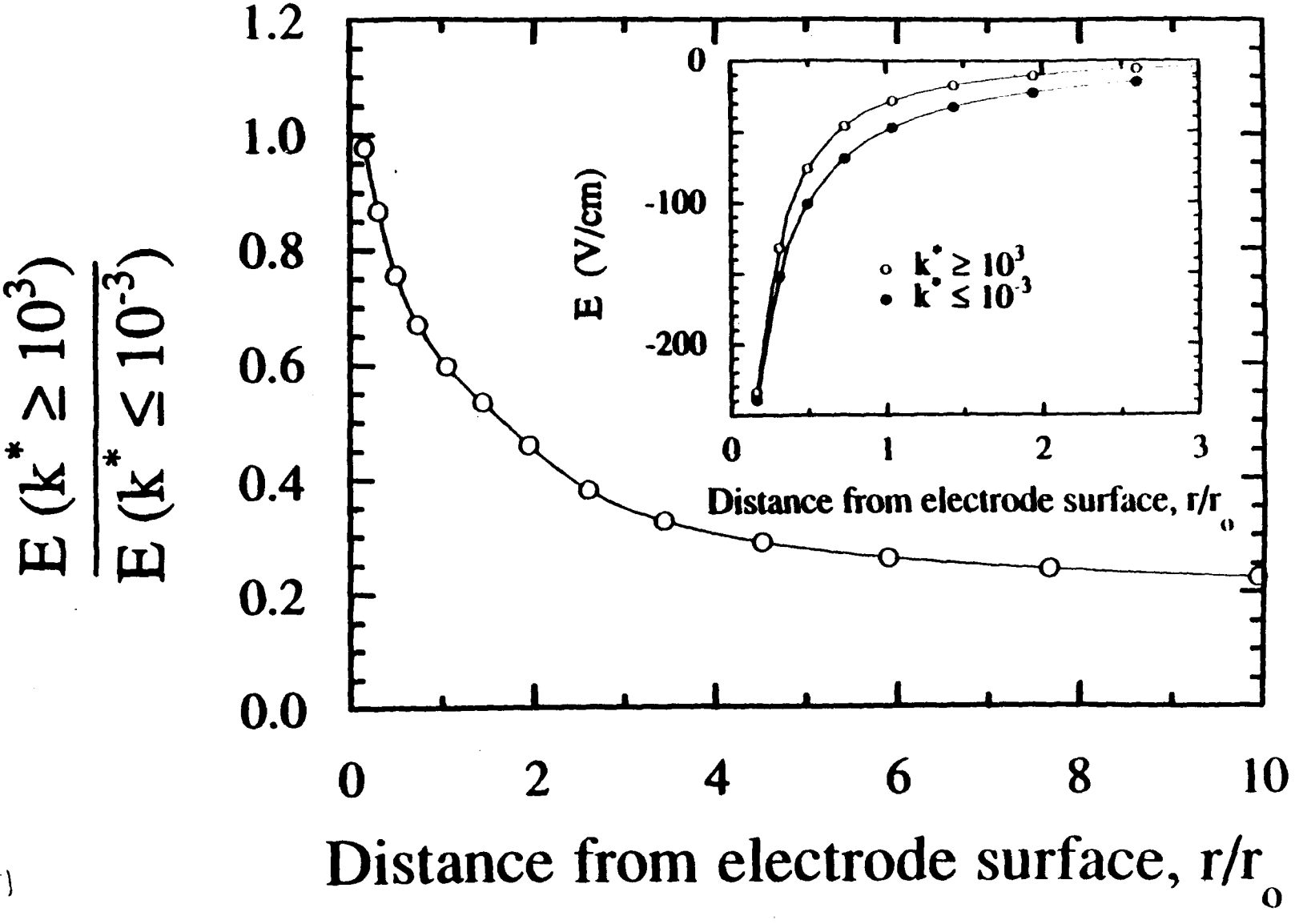
$\frac{E(k^* \geq 10^3)}{E(k^* \leq 10^{-3})}$
1.2
1.0
0.8
0.6
0.4
0.2
0.0
0
2
4
6
8
10
Distance from electrode surface, r/r_o
E (V/cm)
0
-100
-200
$k^* \geq 10^3$
$k^* \leq 10^{-3}$
0
1
2
3
Distance from electrode surface, r/r_o

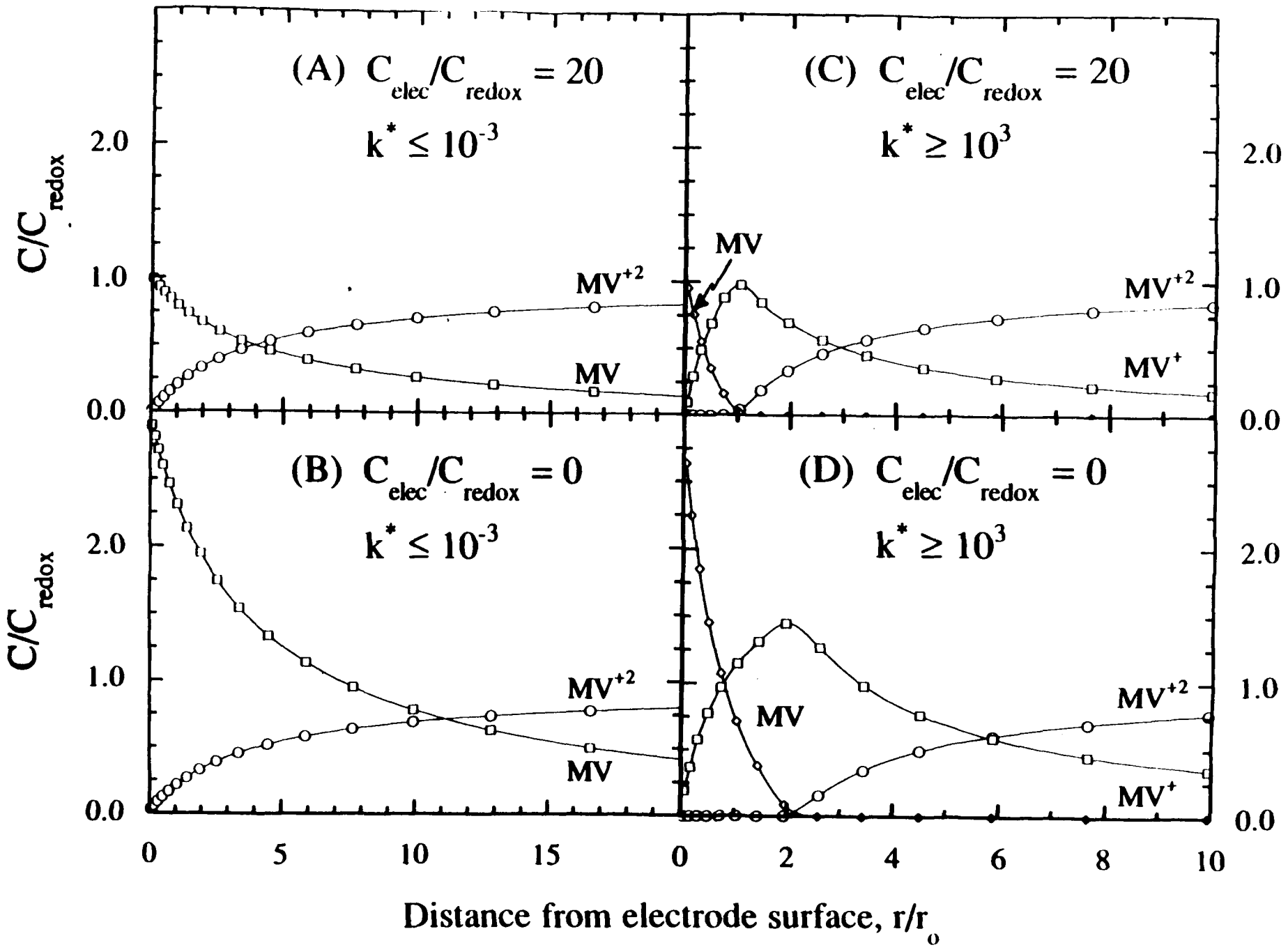
(A) $C_{elec}/C_{redox} = 20$
$k^* \leq 10^{-3}$
(C) $C_{elec}/C_{redox} = 20$
$k^* \geq 10^3$
(B) $C_{elec}/C_{redox} = 0$
$k^* \leq 10^{-3}$
(D) $C_{elec}/C_{redox} = 0$
$k^* \geq 10^3$
MV^{+2}
MV
MV^+
C/C_{redox}
Distance from electrode surface, r/r_o
0.0
1.0
2.0
0
5
10
15
2
4
6
8

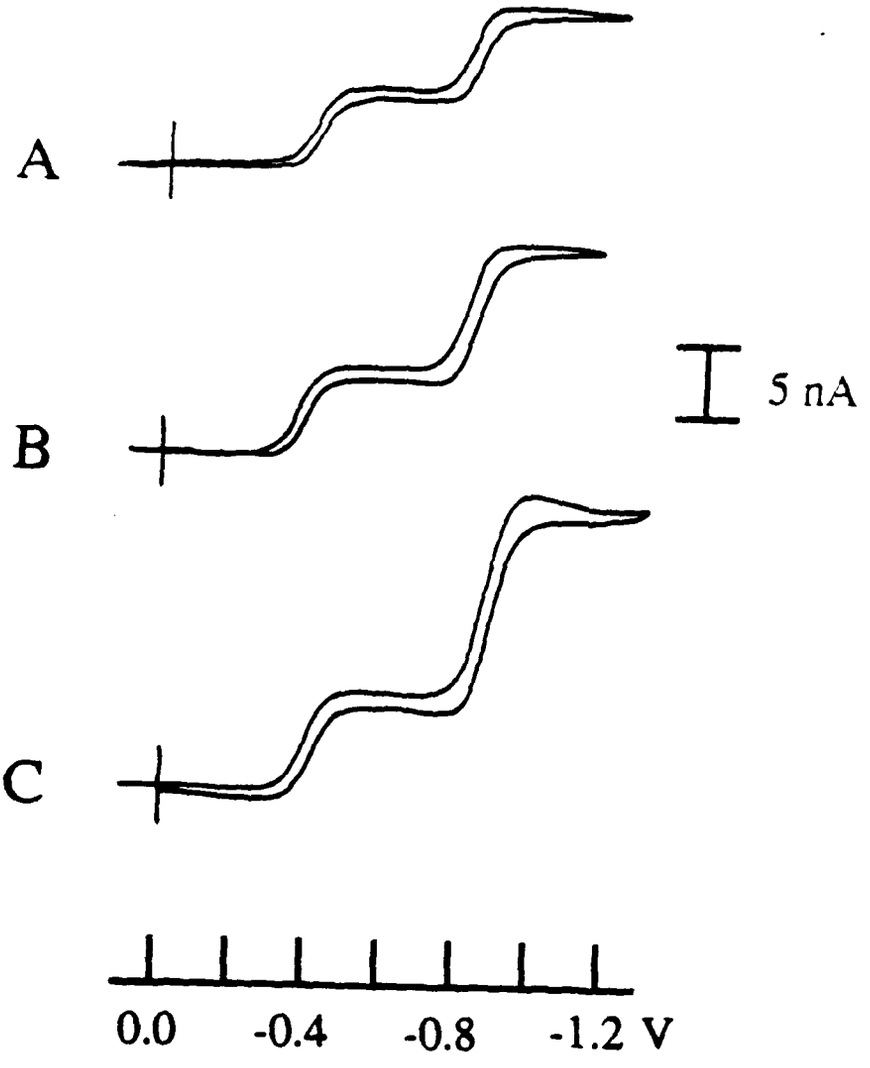

Fig 1

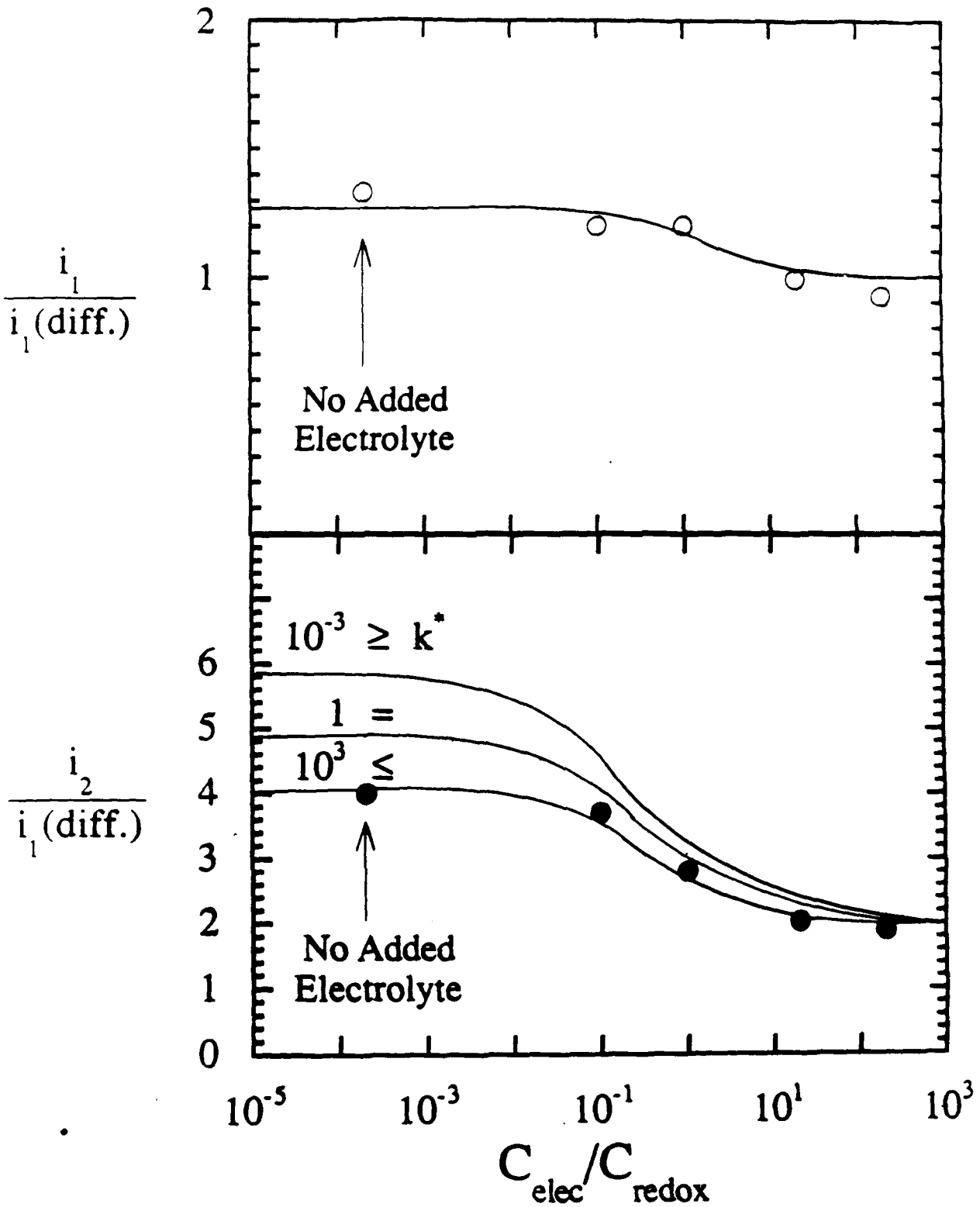
2
1
$\frac{i_l}{i_l(\text{diff.})}$
No Added
Electrolyte
$10^{-3} \geq k^*$
$1 =$
$10^{3} \leq$
6
5
4
3
2
1
0
$\frac{i_2}{i_l(\text{diff.})}$
No Added
Electrolyte
10^{-5}
10^{-3}
10^{-1}
10^{1}
10^{3}
C_{elec}/C_{redox}

Fig 2